ORIGINAL ARTICLE

Agreement between Two Swept-source Optical Coherence Tomography: Optic Nerve Head, Retinal Nerve Fiber Layer and Ganglion Cell Layers in Healthy Eyes

Angelica M Prada[1], Alejandro Tello[2], Carlos M Rangel[3], Virgilio Galvis[4], Gustavo Espinoza[5]

Received on: 13 April 2023; *Accepted on:* 01 June 2023; *Published on:* 10 July 2023

Abstract

Aim and background: Precision of optical coherence tomography (OCT) measurements of the optic nerve head (ONH), retinal nerve fiber layer (RNFL), and macular ganglion cell layer (GCL) is essential for the diagnosis and monitoring of glaucoma. The purpose of this research was to evaluate the repeatability and reproducibility of retinal and ONH parameters measured with two identical swept-source optical coherence devices.

Methods: A cross-sectional study was conducted. A total of 30 eyes of 15 healthy subjects were included. Two technicians performed four OCT-wide protocol scans in the same visit using two identical Triton swept-source OCT (DRI-OCT) instruments. The interdevice and interobserver reproducibility and the repeatability of both instruments for all ONH, RNFL, and macular GCL parameters were evaluated by the intraclass correlation coefficient (ICC). Additionally, Bland–Altman test analysis was used for repeatability and reproducibility measurements.

Results: Intraclass correlation coefficient (ICCs) of the ONH, RNFL, and GCL measurements were excellent for repeatability and interdevice reproducibility (>0.9). Interobserver reproducibility was good for all parameters except for RNFL clock hour 11 (ICC = 0.72). The variability of the average RNFL was from −4.103 to 4.97 µm, with a mean percentage of the difference (PD) of 0.37 ± 2.03%. Among GCL parameters, the greatest variability was found in the inferior sector (PD = −0.88 ± 5.39%, limits of agreement (LoA) = −8.345–7.078 µm).

Conclusion: Using two identical swept-source OCT instruments for the evaluation of the structural parameters of the ONH, RNFL, and macular GCL showed high repeatability and reproducibility. This allows the clinician to make a therapeutic decision based on OCT findings coupled with the clinical evaluation of the patient. When evaluating RNFL clock hours measurements, interobserver reproducibility might decrease.

Clinical significance: The understanding of measurement variability while using different devices and the impact of the observer capturing the images, is clinically relevant.

Keywords: Ganglion cell, Glaucoma, Optical coherence tomography, Optic nerve, Repeatability, Reproducibility, Swept source.

Journal of Current Glaucoma Practice (2023): 10.5005/jp-journals-10078-1409

Introduction

Glaucoma is defined as a chronic, progressive, usually bilateral, and asymmetric optic neuropathy with specific changes in the optic nerve head (ONH), the retinal nerve fiber layer (RNFL), and the visual field.[1] The underlying pathophysiological process is the loss of retinal ganglion cells (RGC).[2] Usually, by the time a glaucomatous visual defect is detected, approximately 28% of the RGC and 17% of the RNFL thickness have been irreversibly damaged.[3,4]

As our understanding of glaucoma has evolved, so has the technology. Optical coherence tomography (OCT) has continued to add parameters to aid in the detection and management of glaucoma. Currently, the peripapillary RNFL is a very important measure for the clinical diagnosis of this entity.[5,6] However, the detection of macular ganglion cell layer (GCL) damage has recently been considered essential, and its changes have been regarded as useful in the early diagnosis of the disease.[7–10]

A new generation of OCT, the swept-source OCT (SS-OCT), was recently introduced. SS-OCT uses a longer wavelength (usually 1050 nm) compared to spectral-domain OCT (SD-OCT). This not only enables the evaluation of RNFL and macular thickness but also allows for high-grade imaging of deeper ocular structures. Additionally, SS-OCT has the advantage of faster scanning speeds (100.000–200.000 A-scans/second), which allows the capture of larger areas in less time.[11]

[1,4,5]Centro Oftalmologico Virgilio Galvis, Floridablanca, Colombia; Department of Ophthalmology, Fundacion Oftalmologica de Santander (FOSCAL), Floridablanca, Colombia; Department of Ophthalmology, Universidad Autonoma de Bucaramanaga (UNAB), Bucaramanga, Colombia

[2,3]Centro Oftalmologico Virgilio Galvis, Floridablanca, Colombia; Department of Ophthalmology, Fundacion Oftalmologica de Santander (FOSCAL), Floridablanca, Colombia; Department of Ophthalmology, Universidad Autonoma de Bucaramanaga UNAB, Bucaramanga, Colombia; Department of Ophthalmology, Universidad Industrial de Santander (UIS), Bucaramanga, Colombia

Corresponding Author: Gustavo Espinoza, Centro Oftalmologico Virgilio Galvis, Floridablanca, Colombia; Department of Ophthalmology, Fundacion Oftalmologica de Santander (FOSCAL), Floridablanca, Colombia; Department of Ophthalmology, Universidad Autonoma de Bucaramanaga (UNAB), Bucaramanga, Colombia Phone: +573162225620, e-mail: drgustavoespinoza@hotmail.com

How to cite this article: Prada AM, Tello A, Rangel CM, *et al.* Agreement between Two Swept-source Optical Coherence Tomography: Optic Nerve Head, Retinal Nerve Fiber Layer and Ganglion Cell Layers in Healthy Eyes. J Curr Glaucoma Pract 2023;17(2):85–90.

Source of support: Nil

Conflict of interest: None

Consistency in the measurements of retinal and ONH parameters with the OCT is essential for the diagnosis, follow-up, and management of glaucomatous and nonglaucomatous optic neuropathies. Previous studies have focused on evaluating the reproducibility of these measurements with a single instrument, assuming that this would be the same with other devices of the same commercial brand. However, there are no studies that have compared the degree of agreement between two identical OCT instruments. The aim of this study was to evaluate the repeatability and reproducibility of retinal and ONH parameters measured with two identical SS-OCT devices.

Methods

We conducted a cross-sectional study in healthy subjects at Centro Oftalmológico Virgilio Galvis in Bucaramanga, Colombia. The study was approved by the ethics committee of Fundación Oftalmológica de Santander-Carlos Ardila Lulle. Written informed consent was obtained from all participants before entering the study. Inclusion criteria were age over 18 years, corrected distance visual acuity of 20/40 or better, a refractive error <5 diopters in spherical refraction and <3 diopters of cylindrical refraction, normal visual field on standard automated perimetry, and open-angle based on the Shaffer grading system. Subjects were excluded if there was the presence of media opacity that could limit OCT image quality, retinal or neurologic disease, and any ocular disease other than incipient cataract, mild blepharitis, or mild dry eye. In addition, subjects with a history of corneal or intraocular surgery were excluded. All participants underwent a detailed ophthalmologic evaluation with a medical history, refraction, and visual acuity measurement with and without correction, slit-lamp evaluation, Goldmann applanation tonometry, gonioscopy, dilated fundoscopy, standard automated perimetry and axial length measurement with an optical ocular biometer IOL master 700, Zeiss, Germany.

Commercially available SS-OCT (DRI OCT Triton; Topcon Corporation, Tokyo, Japan) was used for all examinations. This device uses a central wavelength of 1050 nm with an axial resolution of 8 µm, a transverse resolution of 20 µm, and a capture speed of 100.000 A-scans per second. During imaging, the subject was instructed to fixate on an internal fixation target with particular attention to position on the chin rest and headband. OCT was performed using the 12 x 9 mm 3D wide capture protocol with a resolution of 512 × 256. This protocol allows for the ONH, the peripapillary RNFL, and the GCL to be obtained in the same capture.

All exams were performed by two trained technicians with two different Triton swept-source OCT (DRI-OCT) devices in a single visit. The OCT was taken twice by each technician on each DRI-OCT instrument, meaning that each eye had eight observations (four by each technician) to assess repeatability. Reproducibility was assessed between the DRI-OCT devices (interdevice reproducibility) and between the two trained technicians (interobserver reproducibility). After each capture, the subject was asked to rest and blink. Artifactual images were excluded to avoid poor-quality images. Scans with image quality under 40 were repeated. Measurements of the average RNFL thickness, RNFL by quadrants, and 12 clock hours sectors were considered for the analysis. Likewise, the topographical data of the ONH was evaluated. Regarding the macular GCL, the scan provides two different thickness profiles: the between RNFL and the limits of the inner nuclear layer, including the latter (GCL+) and between the ILM and the limits of the inner nuclear layer, then also including the RNFL (GCL++). Both were evaluated.

Stata/MP 14.1 for Mac was used for data analysis. The sample size calculation was performed using the SAMPCCI software for Stata. With four measurements taken for each eye, a power of 80%, and a statistical significance of 0.05, the estimated sample size was 22 eyes. The distribution of frequencies was determined with the Shapiro–Wilk test. Mean, and standard deviation (SD) are shown unless stated otherwise. Repeatability (test-retest reliability) was tested with estimates of the intraclass correlation coefficient (ICC) and its 95% confidence intervals (95% CI) based on a single-measurement two-way mixed-effects model with absolute agreement. Reproducibility between the two trained technicians (interobserver reproducibility) was tested with estimates of ICC and its 95% CI based on a mean two-way random effects model and absolute agreement. Reproducibility between both DRI-OCT, DRI-OCT 1, and DRI-OCT 2 (interdevice reproducibility) was tested with estimates of ICC and its 95% CI based on a single rater, 2-way mixed-effects model and absolute agreement. ICCs above 0.9 were rated excellent, between 0.9 and 0.8 good, between 0.8 and 0.6 fair, and below 0.6 poor. In addition, Bland–Altman limits of agreement (LoA) and mean percentage of difference (PD) with their SD were measured. All tests were made using generalized estimated equations to avoid the effect of correlation between both eyes of the same patient.

Results

A total of 30 eyes of 15 healthy subjects with a mean age of 29.86 ± 1.11 years (range, 23–43 years), 60% of them women, were studied. The mean spherical equivalent was −0.50 ± 0.68 diopters (range from −2.00 to 0). The mean axial length was 23.52 ± 0.77 mm (range 22.45–24.92 mm), and the mean intraocular pressure was 14.33 ± 3.11 mm Hg (range 10–23 mm Hg).

The average RNFL thickness was 110.87 ± 11.54 µm, being thicker in the inferior quadrant (145 ± 21.95 µm). The mean size of the disc area was 2.09 ± 0.33 mm^2. Regarding the GCL analysis, the sector with the greatest thickness in the GCL++ was the inferonasal, and in the GCL+ was the superonasal, with thicknesses of 121.8 ± 10.47 µm and 76.09 ± 6.64 µm, respectively.

Repeatability

The measurements of the peripapillary RNFL in average quadrants and clock-hour sectors showed excellent repeatability (Table 1). Likewise, all the morphometric parameters of the ONH showed high repeatability (Table 1). The ICCs of the GCL+ and GCL++ were also excellent (Table 1). The lower limit of the 95% CI for the ICC evaluating RNFL, GCL, and ONH showed values above 0.9. Regarding the RNFL, the lowest variability was found in the average RNFL (PD = 0.37 ± 2.03%, LoA = −4.103–4.97 µm), followed by the inferior quadrant (PD = 0.32 ± 2.97%, LoA = −9.444–9.977 µm). Additionally, when evaluating RNFL thicknesses of clock hour sectors, clock hours 3, 4, 5, 8, 9, and 10 showed the lowest variability. Morphometric parameters of the ONH showed less variability for rim area and disc area and greater variability for cup/disc ratio and rim volume measurements. Regarding the GCL+, the greatest variability was found in the inferior sector (PD = −0.88 ± 5.39%, LoA = −8.345–7.078 µm). Within the GCL++ sectors, variability was low with LoA of <3.24 µm.

Interdevice Reproducibility

The RNFL, ONH, and macular GCL showed excellent reproducibility with ICC values above 0.9 for each of the parameters studied

Table 1: Repeatability and reproducibility of the optic nerve, RNFL, and GCL measurements

		Repeatability			*Interobserver*			*Interdevice*		
	Mean ± SD	*ICC*	*% Difference ± SD*	*LOA*	*ICC*	*% Difference ± SD*	*LOA*	*ICC*	*% Difference ± SD*	*LOA*
Average	110.879 ± 11.544	0.986 (0.975–0.993)	0.37 ± 2.03%	−4.103–4.97	0.984 (0.964–0.993)	−0.47 ± 1.78%	−4.61–3.543	0.985 (0.970–0.993)	−2.13 ± 1.74%	−6.231–1.564
Quadrants										
S	137.304 ± 15.452	0.956 (0.926–0.977)	0.57 ± 4.01%	−10.225–12.091	0.970 (0.937–0.986)	0.19 ± 3.16%	−8.63–9.363	0.966 (0.931–0.984)	−2.56 ± 2.95%	−11.415–4.681
I	145 ± 21.95	0.978 (0.963–0.989)	0.32 ± 2.97%	−9.444–9.977	0.969 (0.935–0.985)	-0.62%±3.46%	−11.703–9.303	0.972 (0.941–0.986)	−1.92 ± 3.21%	−13.017–7.217
T	76.588 ± 10.855	0.929 (0.881–0.962)	1.15 ± 6.85%	−9.025–10.625	0.985 (0.968– 0.993)	-0.81%±2.29%	−3.976–2.909	0.968 (0.934–0.985)	−0.95 ± 3.70%	−6.203–4.737
N	84.496 ± 13.191	0.931 (0.884–0.963)	−2.43 ± 8.99%	−15.773–11.906	0.896 (0.783– 0.951)	−2.49 ± 6.79%	−12.95–8.75	0.914 (0.828–0.958)	−3.73 ± 6.70%	−13.764–7.631
Hours										
12	131.996 ± 19.782	0.930 (0.883–0.963)	−0.03 ± 6.02%	−15.408–15.542	0.937 (0.872– 0.970)	−0.02 ± 6.54%	−17.098–16.765	0.931 (0.861–0.967)	−2.83 ± 5.45%	−17.433–10.433
1	130.967 ± 21.386	0.933 (0.887–0.964)	0.85 ± 4.96%	−12.136–14.936	0.821 (0.653–0.912)	−0.86 ± 9.82%	−25.725–23.858	0.933 (0.864–0.968)	−3.17 ± 6.59%	−19.616–11.816
2	107.679 ± 18.457	0.954 (0.922–0.976)	−0.05 ± 6.30%	−13.358–12.825	0.927 (0.851–0.965)	−0.58 ± 6.81%	−14.538–12.938	0.958 (0.914–0.980)	−2.10 ± 4.84%	−12.493–7.893
3	67.058 ± 14.536	0.984 (0.972–0.991)	−0.46 ± 3.23%	−4.557–3.89	0.985 (0.967 – 0.993)	−1.08 ± 3.69%	−5.088–3.488	0.985 (0.969–0.993)	−2.35 ± 3.75%	−6.414–3.28
4	80.021 ± 17.27	0.959 (0.930–0.978)	0.82 ± 4.50%	−6.011–7.345	0.915 (0.825– 0.959)	−2.87 ± 8.51%	−15.663–10.797	0.951 (0.900–0.976)	−3.01 ± 6.89%	−12.82–8.087
5	128.125 ± 27.284	0.982 (0.969–0.991)	0.30 ± 4.15%	−12.132–12.065	0.858 (0.722–0.931)	−2.35 ± 9.82%	−31.521–24.321	0.982 (0.963–0.991)	−1.73 ± 3.92%	−12.288–7.154
6	155.125 ± 29.67	0.969 (0.947–0.984)	0.80 ± 4.49%	−14.57–15.97	0.962 (0.921–0.982)	−0.46 ± 5.01%	−17.396–14.862	0.967 (0.933–0.984)	−2.77 ± 4.28%	−18.949–10.282
7	151.154 ± 24.915	0.966 (0.942–0.982)	−0.18 ± 2.61%	−7.684–7.284	0.811 (0.637–0.907)	1.31 ± 10.51%	−28.118–31.518	0.949 (0.896–0.976)	−1.02 ± 5.27%	−17.219–14.153
8	74.875 ± 12.389	0.959 (0.930–0.978)	−1.24 ± 3.36%	−5.542–3.742	0.869 (0.740–0.936)	0.65 ± 8.47%	−11.556–12.689	0.955 (0.907–0.978)	−1.90 ± 4.81%	−8.672–6.072
9	62.779 ± 8.168	0.970 (0.948–0.984)	−0.17 ± 3.23%	−4.287–3.954	0.966 (0.929–0.984)	−1.15 ± 3.53%	−5.251–3.918	0.975 (0.948–0.988)	−1.55 ± 3.10%	−4.551–2.617
10	92.042 ± 14.342	0.973 (0.953–0.986)	−0.07 ± 2.94%	−5.671–5.404	0.964 (0.925–0.983)	−0.84 ± 3.91%	−8.123–6.523	0.979 (0.956–0.990)	−1.20 ± 3.42%	−7.123–4.723
11	148.925 ± 19.475	0.954 (0.922–0.976)	0.67 ± 4.07%	−11.728–13.862	0.721 (0.488–0.859)	1.63 ± 10.58%	−25.631–29.898	0.966 (0.930–0.984)	−1.45 ± 3.41%	−12.744–8.011
Optic nerve										
DA	2.096 ± 0.332	0.969 (0.946–0.983)	0.25 ± 3.60%	−0.132–0.141	0.963 (0.923–0.982)	−1.06 ± 4.15%	−0.196–0.152	0.968 (0.933–0.984)	−0.58 ± 3.93%	−0.182–0.154
RA	1.472 ± 0.502	0.989 (0.980–0.994)	0.09 ± 4.44%	−0.117–0.124	0.988 (0.975–0.994)	−1.16 ± 5.45%	−0.167–0.134	0.990 (0.980–0.995)	−1.19 ± 4.45%	−0.159–0.12
CDH	0.503 ± 0.213	0.997 (0.995–0.998)	0.63 ± 6.02%	−0.027–0.029	0.997 (0.994–0.999)	−0.32 ± 4.55%	−0.033–0.033	0.997 (0.994–0.999)	0.38 ± 4.24%	−0.029–0.033
CDV	0.489 ± 0.191	0.985 (0.975–0.992)	2.64 ± 12.06%	−0.047–0.063	0.987 (0.973–0.994)	−0.22 ± 9.33%	−0.062–0.064	0.986 (0.970–0.993)	−1.49 ± 8.46%	−0.067–0.061
RV	0.125 ± 0.141	0.992 (0.987–0.996)	2.34 ± 36.33%	−0.041–0.049	0.997 (0.993–0.998)	−4.47 ± 21.13%	−0.022–0.024	0.997 (0.993–0.998)	−3.89 ± 14.71%	−0.025–0.022
GCL ++										
S	111.058 ± 8.87	0.985 (0.974–0.992)	−0.09 ± 1.43%	−3.246–3.046	0.987 (0.969–0.994)	−0.61 ± 1.37%	−3.752 – 2.352	0.986 (0.971–0.993)	−1.68 ± 1.36%	−4.703–1.036
SN	121.796 ± 9.57	0.989 (0.981–0.994)	−0.28 ± 1.14%	−3.024–2.358	0.989 (0.977–0.995)	−0.37 ± 1.15%	-3.177–2.244	0.991 (0.982–0.996)	−1.45 ± 1.01%	−4.218–0.685
ST	95.842 ± 6.39	0.975 (0.957–0.987)	−0.03 ± 1.27%	−2.474–2.407	0.977 (0.953–0.989)	−0.05 ± 1.50%	−2.883–2.749	0.978 (0.954–0.989)	−0.95 ± 1.41%	−3.492–1.692
I	108.204 ± 10.41	0.991 (0.984–0.995)	−0.11 ± 1.46%	−3.21–2.943	0.990 (0.978–0.995)	−0.14 ± 1.35%	−3.084–2.684	0.992 (0.983–0.996)	−1.92 ± 1.34%	−4.632–0.565
IN	121.8 ± 10.477	0.991 (0.985–0.995)	0.17 ± 0.97%	−2.125–2.525	0.988 (0.973–0.995)	−0.59 ± 1.26%	−3.776–2.309	0.993 (0.985–0.997)	−0.84 ± 1.03%	−3.414–1.414
IT	98.454 ± 8.142	0.988 (0.979–0.994)	−0.36 ± 1.22%	−2.654–1.988	0.987 (0.973–0.994)	−0.18 ± 1.31%	−2.693–2.359	0.985 (0.969–0.993)	−1.55 ± 1.49%	−4.307–1.307
GCL +										
S	72.379 ± 6.032	0.986 (0.976–0.993)	0.25 ± 1.06%	−1.292–1.692	0.990 (0.979–0.995)	0.11 ± 1.18%	−1.556– 1.756	0.983 (0.964–0.992)	−0.74 ± 1.60%	−2.729–1.729
SN	76.096 ± 6.644	0.989 (0.981–0.994)	−0.16 ± 1.32%	−2.05–1.85	0.985 (0.968–0.993)	−0.06 ± 1.47%	−2.186–2.119	0.985 (0.969–0.993)	−0.99 ± 1.59%	−3.031–1.565
ST	72.017 ± 5.645	0.983 (0.970–0.991)	0.01 ± 1.54%	−2.184–2.184	0.976 (0.950–0.989)	0.12 ± 1.67%	−2.288–2.422	0.982 (0.963–0.991)	0.05 ± 1.48%	−2.056–2.123
I	68.821 ± 6.604	0.929 (0.881–0.962)	−0.88 ± 5.39%	−8.345–7.078	0.992 (0.984– 0.996)	0.15 ± 1.24%	−1.474–1.674	0.983 (0.965–0.992)	−1.82 ± 1.87%	−3.63–1.163
IN	74.846 ± 7.203	0.993 (0.989–0.997)	0.16 ± 1.16%	−1.553–1.82	0.994 (0.988–0.997)	0.04 ± 1.05%	−1.466–1.532	0.994 (0.987–0.997)	−0.65 ± 1.13%	−2.107–1.107
IT	72.642 ± 6.807	0.990 (0.982–0.995)	−0.16 ± 1.48%	−2.181–1.981	0.989 (0.976–0.995)	0.01 ± 1.38%	−1.993–1.993	0.990 (0.979–0.995)	−0.37 ± 1.34%	−2.188–1.655

CDH, horizontal cup disk ratio; CDV, vertical cup disk ratio; DA, disk área; GCL, ganglion cell layer; ICC, intraclass correlation coefficient; I, inferior; IN, inferonasal; IT, inferotemporal; LOA, limits of agreement; RNFL, retinal nerve fiber layer, RA, rim área; RV, rim volume; S, superior; SN, superonasal; ST, superotemporal

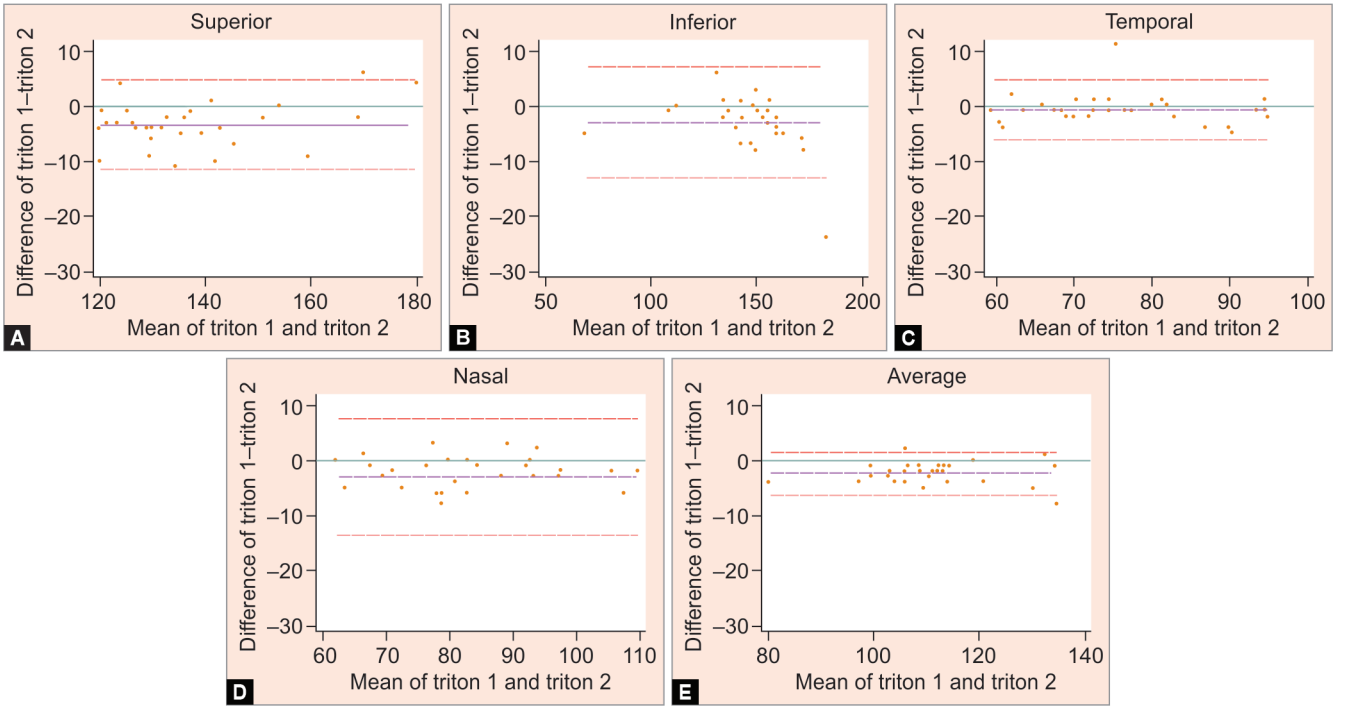

Figs 1A to E: Bland–Altman reproducibility plot for RNFL measurements in average and quadrants

(Table 1). Bland–Altman plots for RNFL average and quadrants are shown in Figure 1. LoA between devices were smaller for average RNFL, followed by temporal, inferior, nasal, and superior, in that order.

Interobserver Reproducibility

The parameters of the peripapillary RNFL showed good reproducibility, with the nasal quadrant showing the lowest ICC with a value of 0.896 (Table 1). Regarding the thickness measurements by clock hour sectors, the reproducibility was good except for clock hour 11, which showed an ICC of 0.721 (95% CI 0.488–0.859). Concerning the data of the ONH and macular GCL parameters, the reproducibility was excellent, with a lower limit of 95% CI for ICC above 0.9 (Table 1).

Discussion

Currently, OCT in glaucoma analysis is a tool that not only serves for diagnosis but also for monitoring the progression of the disease. Being able to demonstrate the repeatability and reproducibility of the measurements obtained with this instrument is of vital importance. These numerical values will allow us to know if the disease is progressing over time and if the treatment that is being carried out is keeping the patient stable from a structural point of view. To know if the measurements of these parameters show variability when using different devices of the same commercial brand is of clinical relevance. In the present study, the ability of SS-OCT to show reproducible data between 2 instruments of the same commercial brand was evaluated.

Our results showed that repeatability and interdevice reproducibility of RNFL, macular GCL, and ONH parameters were excellent. Moreover, interobserver reproducibility of the ONH and macular GCL was excellent for all the evaluated parameters. Regarding RNFL measurements, average and quadrant thicknesses showed good interobserver reproducibility (ICC of >0.8). Several reports have demonstrated the reproducibility of RNFL, GCL, and ONH parameters using SS-OCT with the DRI OCT. Satue et al.[12] investigated the reproducibility of these parameters in healthy subjects using the 12.0 × 9.0 mm 3D wide protocol. Using the ICCs, they found that the parameters with the highest reproducibility were those corresponding to the GCL++ (ICC of >0.90). Unlike our study, the reproducibility of the RNFL parameters was fair to good, with ICC values ranging from 0.685 to 0.946. This greater variability was evidenced even considering that the analysis was not carried out by clock hours but only by six sectors. Regarding the parameters of the ONH, the morphometric data showed good reproducibility.[12] Lee et al. found that repeatability of the parameters of the GCL+ and RNFL using the DRI OCT in healthy Korean subjects was excellent.[13]

In the present study, we evaluated the repeatability and reproducibility of the RNFL in average quadrants and clock hours sectors. Although average and quadrant RNFL measurements showed good reproducibility, among clock hours, good interobserver reproducibility was found in all parameters except for clock hour 11, which showed an ICC of 0.72. Carpineto et al. found that reproducibility using SD-OCT with Cirrus (Carl Zeiss Meditec, Dublin, California, United States of America) was reduced when RNFL was evaluated by clock hours. In their analysis, the RNFL clock hours corresponding to hour 7 showed ICC values of 0.75 and 0.72 with the two operators who carried out the exams.[14] Similarly, Arthur et al. evaluated the reproducibility of the RNFL parameters using time-domain OCT with the Stratus (Carl Zeiss Meditec, Dublin, California, United States of America), finding that when evaluating the ICC of the average RNFL, quadrants and clock hour sectors, the parameters that showed the greatest variability were those corresponding to clock hours. In their study, the sector that showed the lowest ICC was the one corresponding to clock hour 2 with a value of 0.70.[15] One possible explanation for this greater variability in clock hours is the influence of head position during the capture. Hwang et al. demonstrated that OCT measurements with

different degrees of head tilt produced an increase or decrease in RNFL thickness in the clock hour sector.[16]

Since its development, OCT technology has evolved through the years with the capability of obtaining images of higher resolution with newer devices. SS-OCT offers several advantages for image acquisition compared to its predecessors, like faster scan speed and longer wavelength. Despite the technological differences, previous reports have shown that repeatability and the glaucoma diagnostic ability of SS-OCT and SD-OCT are similar. Lee et al. found that both the DRI OCT and Cirrus OCT had excellent repeatability in healthy subjects for measurements of the RNFL and GCL+, with the exception of the temporal clock hour sector of the RNFL in the Cirrus OCT. However, when the repeatability of both instruments was compared, DRI OCT RNFL measurements showed higher values than the Cirrus. Interdevice agreement was more variable than intra-device, with thinner measurements of the GCL+ and thicker measurements of the RNFL in the DRI OCT compared to Cirrus.[13] This finding was previously described in glaucoma patients and healthy subjects confirming that these measurements are not interchangeable for clinical purposes.[17,18] Although the differences in these parameters might be related to technology, they could also be related to the segmentation algorithm. One possible explanation could be that the DRI OCT measures circumpapillary RNFL closer to the diameter of the ONH compared to other companies. In general, as the measurement gets closer to the ONH border, the thickness of the RNFL increases, which could explain this finding. Moreover, something similar occurs with the measurements of the macular GCL, where the thickness decreases as the measurement is further from the fovea. The GCL+ measurement area in the DRI OCT is inside a 6 mm diameter circle around the fovea in contrast to the 4.8 × 4.0 mm of Cirrus.

To our knowledge, this is the first study that evaluates the repeatability and reproducibility of SS-OCT with two devices of the same commercial brand. As limitations, it is worth mentioning that these results can only be applied to healthy subjects since we did not include patients with glaucoma or with high ranges of refractive errors. Another consideration is that these results are valid only in the context of good-quality OCT images. It has already been described that as there is a greater fluctuation in the quality of the OCT images, a relevant reduction in the repeatability of the images can be observed.[19]

We can conclude that the evaluation of the structural parameters of the ONH, RNFL, and GCL have high repeatability and reproducibility even if they are taken by different operators with different instruments of the same commercial brand.

Clinical Significance

This provides greater confidence for the monitoring of diseases such as glaucoma, where the reduction of tissue thickness can be a marker of progression, and in this way, therapeutic approaches can be taken based on OCT findings together with the clinical evaluation of the patient. The most reliable RNFL thickness measurements are those from the average RNFL. Care must be taken when analyzing RNFL clock hours measurements as interobserver reproducibility might decrease with these parameters.

Orcid

Angelica M Prada https://orcid.org/0000-0001-9076-356X
Alejandro Tello https://orcid.org/0000-0001-5081-0720
Carlos M Rangel https://orcid.org/0000-0002-6198-0503
Virgilio Galvis https://orcid.org/0000-0003-4587-5364
Gustavo Espinoza https://orcid.org/0000-0003-2519-2355

References

1. Stamper RL, Lieberman MF, Drake M V. Becker - Shaffer´s Diagnosis and Therapy of the Glaucomas. 8th ed. Mosby/Elsevier; 2009. 561p.
2. Wang AY, Lee PY, Bui BV, et al. Potential mechanisms of retinal ganglion cell type-specific vulnerability in glaucoma. Clin Exp Optom 2020;103(5):562–571. DOI: 10.1111/cxo.13031
3. Medeiros FA, Zangwill LM, Bowd C, et al. Evaluation of retinal nerve fiber layer, optic nerve head, and macular thickness measurements for glaucoma detection using optical coherence tomography. Am J Ophthalmol 2005;139(1):44–55. DOI: 10.1016/j.ajo.2004.08.069
4. Wollstein G, Kagemann L, Bilonick RA, et al. Retinal nerve fibre layer and visual function loss in glaucoma: the tipping point. Br J Ophthalmol 2012;96(1):47–52. DOI: 10.1136/bjo.2010.196907
5. Hammel N, Belghith A, Weinreb RN, et al. Comparing the rates of retinal nerve fiber layer and ganglion cell-inner plexiform layer loss in healthy eyes and in glaucoma eyes. Am J Ophthalmol 2017;178:38–50. DOI: 10.1016/j.ajo.2017.03.008
6. Khanal S, Davey PG, Racette L, et al. Comparison of retinal nerve fiber layer and macular thickness for discriminating primary open-angle glaucoma and normal-tension glaucoma using optical coherence tomography. Clin Exp Optom 2016;99(4):373–381. DOI: 10.1111/cxo.12366
7. Nakanishi H, Akagi T, Hangai M, et al. Sensitivity and specificity for detecting early glaucoma in eyes with high myopia from normative database of macular ganglion cell complex thickness obtained from normal non-myopic or highly myopic Asian eyes. Graefe's Arch Clin Exp Ophthalmol 2015;253(7):1143–1152. DOI: 10.1007/s00417-015-3026-y
8. Kim KE, Jeoung JW, Park KH, et al. Diagnostic classification of macular ganglion cell and retinal nerve fiber layer analysis: differentiation of false-positives from glaucoma. Ophthalmology 2015;122(3):502–510. DOI: 10.1016/j.ophtha.2014.09.031
9. Xu X, Xiao H, Guo X, et al. Diagnostic ability of macular ganglion cell-inner plexiform layer thickness in glaucoma suspects. Medicine (Baltimore) 2017;96(51):e9182. DOI: 10.1097/MD.0000000000009182
10. Shin JW, Sung KR, Lee GC, et al. Ganglion cell-inner plexiform layer change detected by optical coherence tomography indicates progression in advanced glaucoma. Ophthalmology 2017;124(10):1466–1474. DOI: 10.1016/j.ophtha.2017.04.023
11. Laíns I, Wang JC, Cui Y, et al. Retinal applications of swept source optical coherence tomography (OCT) and optical coherence tomography angiography (OCTA). Prog Retin Eye Res 2021;84:100951. DOI: 10.1016/j.preteyeres.2021.100951
12. Satue M, Gavin A, Orduna E, et al. Reproducibility and reliability of retinal and optic disc measurements obtained with swept-source optical coherence tomography in a healthy population. Jpn J Ophthalmol 2019;63(2):165–171. DOI: 10.1007/s10384-018-00647-2
13. Lee SY, Bae HW, Kwon HJ, et al. Repeatability and agreement of swept source and spectral domain optical coherence tomography evaluations of thickness sectors in normal eyes. J Glaucoma 2017;26(2):e46–e53. DOI: 10.1097/IJG.0000000000000536
14. Carpineto P, Nubile M, Agnifili L, et al. Reproducibility and repeatability of Cirrus™ HD-OCT peripapillary retinal nerve fibre layer thickness measurements in young normal subjects. Ophthalmologica 2012;227(3):139–145. DOI: 10.1159/000334967
15. Arthur SN, Smith SD, Wright MM, et al. Reproducibility and agreement in evaluating retinal nerve fibre layer thickness between Stratus and Spectralis OCT. Eye (Lond) 2011;25(2):192–200. DOI: 10.1159/000334967
16. Hwang YH, Lee JY, Kim YY. The effect of head tilt on the measurements of retinal nerve fibre layer and macular thickness by spectral-domain optical coherence tomography. Br J Ophthalmol 2011;95(11):1547–1551. DOI: 10.1136/bjo.2010.194118
17. Yang CM, Lim DH, Kim HJ, et al. Comparison of two swept-source optical coherence tomography biometers and a partial coherence

interferometer. PLoS One 2019;14(10):e0223114. DOI: 10.1371/journal.pone.0223114
18. Yang Z, Tatham AJ, Zangwill LM, et al. Diagnostic ability of retinal nerve fiber layer imaging by swept-source optical coherence tomography in glaucoma. Am J Ophthalmol 2015;159(1):193–201. DOI: 10.1016/j.ajo.2014.10.019
19. Yang H, Lee HS, Bae HW, et al. Effect of image quality fluctuations on the repeatability of thickness measurements in swept-source optical coherence tomography. Sci Rep 2020;10(1):13897. DOI: 10.1038/s41598-020-70852-y